Ann. Geophys., 35, 721–731, 2017
https://doi.org/10.5194/angeo-35-721-2017

Annales Geophysicae Open Access EGU

Atmospheric loss from the dayside open polar region and its dependence on geomagnetic activity: implications for atmospheric escape on evolutionary timescales

Rikard Slapak[1], **Audrey Schillings**[1,2], **Hans Nilsson**[1,2], **Masatoshi Yamauchi**[2], **Lars-Göran Westerberg**[3], **and Iannis Dandouras**[4,5]

[1]Division of Space Technology, Luleå University of Technology, Kiruna, Sweden
[2]Swedish Institute of Space Physics, Kiruna, Sweden
[3]Division of Fluid and Experimental Mechanics, Luleå University of Technology, Luleå, Sweden
[4]CNRS, Institut de Recherche en Astrophysique et Planétologie, Toulouse, France
[5]University of Toulouse, UPS-OMP, IRAP, Toulouse, France

Correspondence to: Rikard Slapak (rikard.slapak@ltu.se)

Received: 14 January 2017 – Revised: 3 May 2017 – Accepted: 10 May 2017 – Published: 12 June 2017

Abstract. We have investigated the total O^+ escape rate from the dayside open polar region and its dependence on geomagnetic activity, specifically Kp. Two different escape routes of magnetospheric plasma into the solar wind, the plasma mantle, and the high-latitude dayside magnetosheath have been investigated separately. The flux of O^+ in the plasma mantle is sufficiently fast to subsequently escape further down the magnetotail passing the neutral point, and it is nearly 3 times larger than that in the dayside magnetosheath. The contribution from the plasma mantle route is estimated as $\sim 3.9 \times 10^{24} \exp(0.45\,\mathrm{Kp})$ [s^{-1}] with a 1 to 2 order of magnitude range for a given geomagnetic activity condition. The extrapolation of this result, including escape via the dayside magnetosheath, indicates an average O^+ escape of $3 \times 10^{26}\,\mathrm{s}^{-1}$ for the most extreme geomagnetic storms. Assuming that the range is mainly caused by the solar EUV level, which was also larger in the past, the average O^+ escape could have reached $10^{27–28}\,\mathrm{s}^{-1}$ a few billion years ago. Integration over time suggests a total oxygen escape from ancient times until the present roughly equal to the atmospheric oxygen content today.

Keywords. Magnetospheric physics (magnetosheath; solar wind and magnetosphere interactions; storms and substorms)

1 Introduction

Investigations of terrestrial ion outflow and escape and its dependence on geomagnetic activity are important in order to obtain an increased understanding of magnetospheric dynamics, but also from an atmospheric evolution point of view. In the young solar system, the Sun is believed to have been more active (e.g. Ribas et al., 2005; Güdel, 2007) with a higher EUV flux, higher solar wind dynamic pressure, and a more intense and active magnetic field (solar dynamo) due to faster rotation (Wood, 2006; Airapetian and Usmanov, 2016). This indicates that the young Earth experienced more intense geomagnetic activity compared to the present time (Krauss et al., 2012) and hence high escaping fluxes of ionospheric ions (Moore et al., 1999; Cully et al., 2003; Peterson et al., 2008).

Ionospheric outflows typically originate at high latitudes, either along the closed field lines of the auroral region, directly feeding the plasma sheet, or along the open magnetic field lines of the polar cap and cusp. A review of high-latitude ionospheric outflow is given by Yau and André (1997). Outflow along open field lines will generally be put on trajectories leading tailward, and its fate is to a high degree determined by the energisation along the path. Cold (< 1 eV) H^+ and O^+ outflows can thus dominate in both flux and density in the distant magnetotail lobes (Engwall et al., 2009). The cusps are regions which enable direct interaction between the magnetosheath and the ionosphere, leading to increased elec-

tron temperatures and higher ion upflows as a consequence in the cusp ionosphere (Nilsson et al., 1996; Ogawa et al., 2003; Kistler et al., 2010). Ionospheric upflow is still gravitationally bound and needs further energisation in order to reach the magnetosphere. The act of the mirror force converts perpendicular energy into parallel energy for upflowing ions moving into regions of weaker magnetic field, and thus the perpendicular heating of plasma indirectly leads to acceleration along the field lines. Several studies have investigated this and shown that wave–particle interaction is effective in ion transverse heating over the whole range of altitudes in the cusps (André et al., 1990; Norqvist et al., 1996; Bouhram et al., 2003; Waara et al., 2011; Slapak et al., 2011), and the fate of the cusp ion outflow depends on the energisation of the ions along its path.

One can consider the cusp O^+ outflow to take one of three different main paths (corresponding to the yellow illustrative trajectories in Fig. 1) depending on how effectively it is accelerated: (1) low-energised ion populations will convect anti-sunward across the polar cap and further downtail and towards the plasma sheet, where they end up on closed field lines (Kistler et al., 2010; Liao et al., 2015); (2) sufficiently energised ions will reach the plasma mantle with typical velocities high enough to pass the tail X-line and consequently escape in the distant tail (Nilsson, 2011); (3) highly energised ions may escape into the dayside magnetosheath directly from the cusps (Slapak et al., 2012, 2013). Heavy (e.g. O^+) energetic ions can also escape to the dayside magnetosheath through magnetopause shadowing (Marcucci et al., 2004). Escaping ions during a strong northward interplanetary magnetic field may be brought back into the magnetosphere if dual-lobe reconnection takes place (Song and Russell, 1992). The fraction that might be brought back is, however, a low percentage and its effect on the total escape along route 3 is negligible (Slapak et al., 2015).

It is well known that the ion outflow rates are enhanced during geomagnetically active times. For example, Yau et al. (1988) parameterised the ionospheric ion outflow and found that the O^+ outflow rate increased exponentially with Kp as exp(0.5 Kp). Other studies that have shown a clear correlation between O^+ and geomagnetic activity are Peterson et al. (2001), Cully et al. (2003), and Kistler and Mouikis (2016). The O^+ density close to the mid-latitude magnetopause was shown by Bouhram et al. (2005) to also increase exponentially with Kp. A consequence of increased ion outflow is an enhancement of the plasma feed into the plasma sheet during geomagnetic storms (Nose et al., 2005; Kistler et al., 2010; Haaland et al., 2012). The plasma sheet in turn feeds the ring current and its relative O^+ content and energy density increases significantly with geomagnetic activity. For example, Young et al. (1982) showed that the O^+ / H^+ density ratio increases exponentially with Kp ($\sim$ exp(0.17 Kp)).

We will investigate and quantify the O^+ escape rate and its dependence on geomagnetic activity in two regions associated with ion escape: the plasma mantle and the high-latitude magnetosheath. For the strongest geomagnetic conditions, the statistics become sparse and we need to extrapolate our results in order to say something about atmospheric loss during such events. Specific cases of O^+ outflow and escape during major geomagnetic storms need to be investigated in the future as a complement.

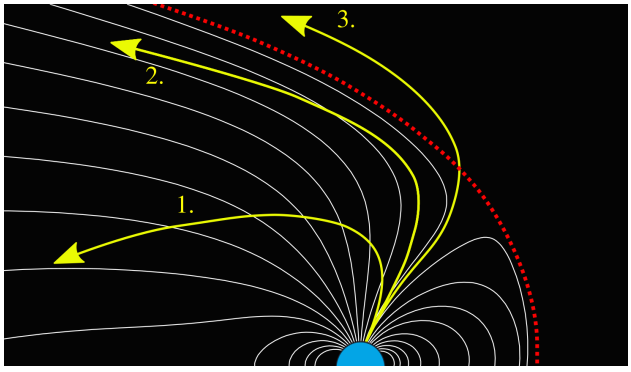

Figure 1. An illustration of possible magnetospheric ion outflow trajectories: (1) low-energy ion transport to the plasma sheet; (2) high-energy ion flows in the plasma mantle leading to escape downstream in the tail; (3) high-energy ion escape directly from the cusp into the high-latitude dayside magnetosheath. The red dashed line illustrates the magnetopause.

2 Instruments and data criteria

In this section, we first describe the instruments that provide us with the necessary data for our study, followed by descriptions of and criteria for the data sets corresponding to the plasma mantle and the high-latitude magnetosheath respectively.

2.1 Instruments

The study presented in this paper uses data obtained by instruments on-board two spacecraft (SC1 and SC4) of the Cluster mission (Escoubet et al., 2001), which consists in total of four spacecraft flying in formation with an identical set of instruments on-board. The composition distribution function (CODIF) spectrometer, described in detail by Rème et al. (2001), has mass resolution and provides ion distributions for different species (for particle energies up to 38 keV q^{-1}) from which the ion moments have been calculated. The magnetic field data are provided by the fluxgate magnetometer (FGM) (Balogh et al., 2001), which in normal mode has a sample frequency of 22.4 Hz. We are interested in the background magnetic field and therefore use field data averaged over the spacecraft spin period of 4 s, as is the ion moment data. The data set used for the plasma mantle statistics was obtained by SC4 and covers 2001–2005. For the high-latitude magnetosheath we use the data set compiled by Slapak et al.

(2013), in which times of high-energy O^+ were visually determined for 2001–2003 for SC1.

2.2 Plasma mantle

In order to study O^+ flows in the plasma mantle, the corresponding data need to be separated from polar cap and magnetosheath data. Figure 2 shows a high-latitude dayside passage of Cluster 1 from the magnetosheath across the magnetopause at around 09:18 UT and into the plasma mantle followed by a gradual decrease in ion flux intensity as it moves into the polar cap. The top and middle panel show the energy spectrograms for H^+ and O^+ respectively, and the bottom panel shows the magnetic field strength and its components. The magnetosheath is often characterised as a more fluctuant magnetic field compared to the field inside the magnetosphere. More importantly, it is also characterised by very strong H^+ fluxes. These intense fluxes cause contamination in the O^+ mass channel, yielding false counts; this contamination can be tracked and removed as described by Nilsson et al. (2006). The polar cap is a region associated with a low-energy ion environment in comparison with the plasma mantle, which is filled with denser energetic mirrored solar wind plasma. As a consequence, the plasma β number, defined as the thermal plasma pressure over magnetic pressure, is typically significantly higher in the plasma mantle. However, there is a gradual transition between the two regions and no distinct β value that will separate them. In statistical studies of the polar cap, data with the constraint that β is less than 0.01 are used (e.g. Liao et al., 2010, 2015). Therefore, a constraint of $\beta > 0.1$ in the dayside magnetosphere will exclude typical polar cap data. Using a somewhat lower or higher limit for β does not affect the results of this study, and therefore a $\beta > 0.1$ constraint is adopted. A blue rectangle in Fig. 2 marks the interval at which the criteria for the plasma mantle data associated with this particular magnetopause crossing are fulfilled.

We also put regional constraints on the data set by removing the inner magnetosphere ($R_{GSM} = (Y_{GSM}^2 + Z_{GSM}^2)^{1/2} > 6\,R_E$). We also consider data within a range of $-5 < X_{GSM} < 8\,R_E$. This allows for good spatial coverage in the dusk–dawn extent as well as sufficient data during the highest geomagnetic activities (high Kp). The results and conclusions of the study presented in this paper are not very sensitive to these exact limits, but they can be slightly altered.

However, the β and regional constraints are not sufficient. In Fig. 3, the H^+ (blue bars) and O^+ (red) perpendicular temperatures and number densities for $\beta > 0.1$ are presented. Panels (a) and (d) (top panels) show the distribution for all $\beta > 0.1$ data. In the H^+ data there are two clearly distinct peaks: around a few hundred eV and a few thousand eV for the temperature, and around 0.3 and 10 cm^{-3} for the density, suggesting two distinct plasma populations within our data set. We investigate this by separating the data into two subsets of $T_\perp(H^+) < T_{cut}$ and $T_\perp(H^+) > T_{cut}$ with $T_{cut} = 1750$ eV, marked in panel (a) as a vertical black dot-dashed line. The data corresponding to H^+ perpendicular temperatures larger than T_{cut} are shown in panels (b) and (e) (middle panels), and the data corresponding to the lower H^+ perpendicular temperatures are shown in panels (c) and (f) (bottom panels). It becomes clear that the data separation with respect to temperature also separates the density data, such that the lower density population relates to the high temperature population and the higher densities to the lower temperature population. This indeed confirms that there are two distinct populations with clear differences in the H^+ characteristics represented in the data set.

The H^+ population with high temperatures and low densities is consistent with the average characteristics of the plasma sheet presented by e.g. Baumjohann et al. (1989) and Kistler et al. (2006), whereas the population of lower temperatures but higher densities is what we expect to observe in the plasma mantle (e.g. Nilsson et al., 2006). The corresponding O^+ data also reveal differences in the characteristics between the two regions. For the plasma-sheet-like population, the O^+ temperatures are about the same as the H^+ temperatures, and the O^+ density is typically 1 order of magnitude lower than the H^+ density; this is consistent with plasma sheet measurements presented by Kistler et al. (2006). In the plasma mantle, however, the O^+ temperature spans a large range, from a few tens of eV up to 10 keV, but is in general considerably lower than for the plasma-sheet-like population. The O^+ density in the plasma mantle is higher than the plasma sheet O^+ densities, but still 1 to 2 orders of magnitude smaller than the corresponding H^+ densities, which is consistent with plasma mantle observations (Nilsson et al., 2012).

For the purpose of investigating O^+ fluxes in the plasma mantle, we constrict the data with the condition $T_\perp(H^+) < 1750$ eV in order to exclude the plasma-sheet-like population. The number of data points corresponding to the plasma mantle is just over 382 000, and the distribution as a function of Kp is shown as blue bars in Fig. 4. Moderate geomagnetic activity is most common, but some data for the highest values of Kp are also available. The number of data points for periods of Kp = 9 is below 100; this is too low to be visible in the chart due to the linear scale, and we leave it out of the statistical analysis.

2.3 The high-latitude magnetosheath

O^+ data in the high-latitude dayside magnetosheath covering 2001 to 2003 were identified by Slapak et al. (2013) through the visual inspection of O^+ energy spectrograms for ion energies larger than 3 keV in order to avoid false counts due to the intense H^+ fluxes in the magnetosheath (Nilsson et al., 2006). The middle panel of Fig. 2 shows such typical magnetosheath high-energy O^+ populations (marked with red rectangles) in the interval up to the magnetopause crossing at ∼ 09:18. Studies of such populations were presented by Slapak et al. (2012), who reported that the pop-

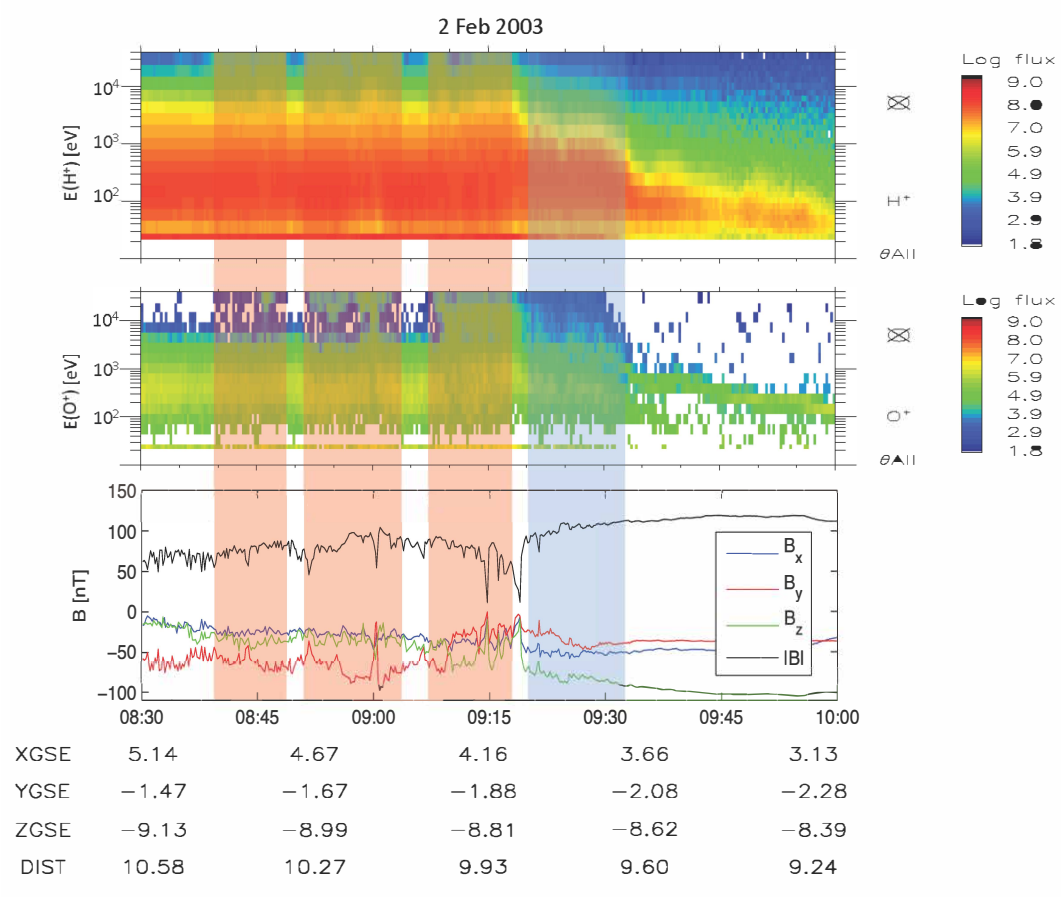

Figure 2. An example of a magnetopause crossing (∼ 09:18 UT) in the southern high-latitude dayside hemisphere with Cluster 1, travelling from the magnetosheath into the plasma mantle and then the polar cap. The first and second panels show the H^+ and O^+ energy spectrograms respectively. The third panel shows the magnetic field strength and its components. The time intervals of the plasma mantle and magnetosheath data included in this study (for this particular time interval) are marked with blue and red rectangles respectively.

ulations had D-shaped velocity distributions, indicating that they had passed through a rotational discontinuity at the magnetopause, which is consistent with escape along open field lines. Only the months January to June were considered when picking out these types of magnetosheath O^+ populations as this period corresponds to a Cluster apogee in the dayside, allowing for regular passages through the high-latitude dayside magnetosheath. This data set allowed Slapak et al. (2013) to estimate an average total anti-sunward O^+ flux of $0.7 \times 10^{25}\,s^{-1}$, corresponding to direct escape from the cusps. In this study, we will use the same data set to study how the total escape from the cusps depends on the geomagnetic activity. The distribution of the O^+ observations in response to geomagnetic activity is shown in Fig. 4, where the magnetosheath data (roughly 92 000 data points) are binned (red bars) according to the simultaneously measured Kp values. Unfortunately, no magnetosheath data for conditions of $Kp \geq 7$ are present in the data set. For $Kp = 6$ we have very few data points, such that the O^+ data are not visible in the figure due to the choice of a linear scale.

3 Observations

Based on the data of the plasma mantle and magnetosheath described in Sect. 2, average fluxes scaled to ionospheric altitudes in order to cancel any altitude dependencies are calculated as a function of Kp. If the total particle flux is assumed to be conserved along a magnetic flux tube, the local particle flux F can be scaled to an ionospheric altitude as $F_I = F B_I / B$, where B_I is the ionospheric magnetic field strength set to 50 000 nT and B is the locally measured field strength. The result is shown in Fig. 5 and reveals a clear increase in flux with increased geomagnetic activity for both the plasma mantle (blue) and the high-latitude dayside magnetosheath (red). The error bars represent the standard deviations and are slightly shifted in the figure for visibility. Note that results are obtained only for $Kp \leq 8$ and ≤ 6 for the plasma mantle regime and the magnetosheath respectively. The fluxes in the plasma mantle typically increase by 1.5 orders of magnitude between quiet times and times of the most extreme geomagnetic conditions. The scaled O^+ flux in the

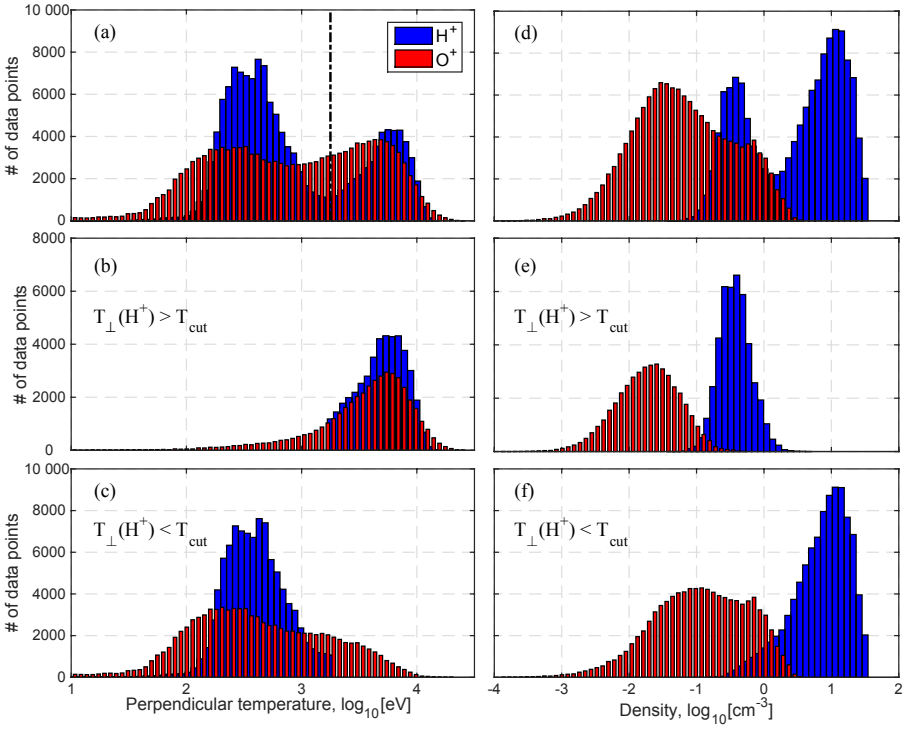

Figure 3. Distributions of $\beta > 0.1$ data in the dayside magnetosphere, covering 2001–2005. The left and right panels represent H^+ and O^+ temperatures and number densities respectively. The top panels **(a, d)** show all data, whereas the middle panels **(b, e)** show the data subset corresponding to H^+ $T_\perp$ higher than $T_{cut} = 1750$ eV, marked with a vertical line in **(a)**. The lower panels show the data subset corresponding to H^+ $T_\perp$ lower than T_{cut}.

magnetosheath is in principle the same as in the plasma mantle, at least up to Kp = 6.

We will estimate the total O^+ flux in the plasma mantle and magnetosheath separately as functions of Kp using the method implemented by Slapak et al. (2013) when calculating the average O^+ escape flux from the cusp into the high-latitude magnetosheath. They divided the data into spatial segments aligned with the magnetosheath high-latitude flow, yielding an escape cross section when also considering an effective outflow region with a dusk–dawn extent of 106° at the highest latitudes. The flow is typically tangential to the magnetopause, and therefore a magnetopause shape model, introduced by Shue et al. (1997), was used to define the stream-aligned segments in which O^+ occurrence rates and average fluxes were used to calculate the total O^+ escape rate. A much more detailed description of the method is given by Slapak et al. (2013). We note that the most significant plasma mantle outflows are at high latitudes as one would expect, and it turns out that the same dusk–dawn extent as observed for the magnetosheath is suitable for the plasma mantle calculations.

The plasma mantle bulk flow is similar to the magnetosheath flow in terms of the magnetopause-aligned flux. The method requires, however, good spatial coverage with significant data points. The most common are times with Kp = 3, followed by Kp = 2 and 4 and then Kp = 1 and 5 (Fig. 4), and the method works fine for data corresponding to these Kp indices individually. However, the amounts of data for Kp = 0, 6, 7, and 8 are too small. We therefore combine the data for Kp = 0 and 1 and let the corresponding escape rate correspond to the average Kp value for this subset. For the highest geomagnetic activity conditions (Kp = (6, 7, 8)), the combined number of data points is even lower. This can be seen in Fig. 6, where the spatial coverage of the plasma mantle O^+ data is shown for different Kp values. However, the spatial coverage for this high geomagnetic activity subset is still decent and the same method can be applied. In the figure, the data are divided into bins of $1 R_E \times 1 R_E$ for which average O^+ fluxes (defined by the colour bar) and bulk velocities (arrows) are determined in order to visualise the spatial coverage and bulk flow. An arrow for reference is in the upper right corner in the first plot (Kp = (0, 1)) and has a length corresponding to 100 km s^{-1}. For clarity, we note that for the estimate of the total escape, we consider the average within each magnetopause tangential segment rather than the averages of the bins.

For the magnetosheath we use the same data set as Slapak et al. (2013). The data cover, as already mentioned, a smaller range of geomagnetic activity and we calculate the O^+ escape rate for Kp = (0, 1), Kp = 2, Kp = 3, and Kp = (4, 5, 6).

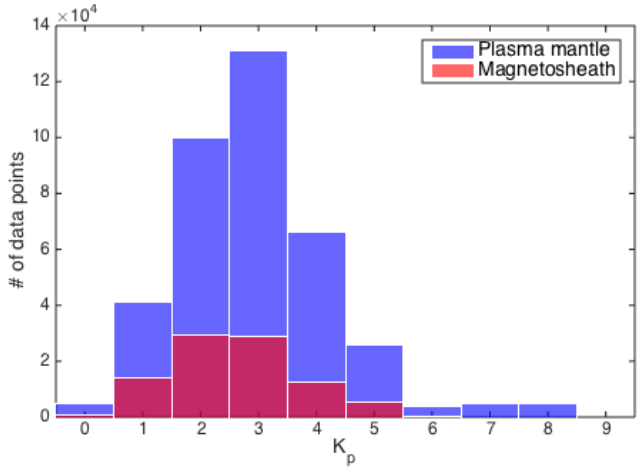

Figure 4. Distribution of O^+ observations over Kp for the plasma mantle (blue) and dayside magnetosheath (red) respectively.

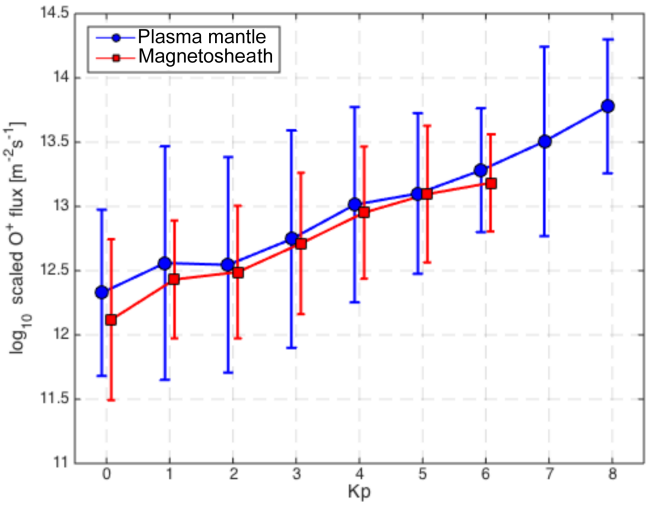

Figure 5. The average O^+ flux measured for the plasma mantle (blue circles) and in the magnetosheath (red squares), scaled to an ionospheric reference altitude as a function of Kp with error bars representing the standard deviations.

The average O^+ escape rates are shown in Fig. 7 as blue (plasma mantle) and red (magnetosheath) solid lines with circles and squares respectively. As expected, the O^+ escape flux increases with higher geomagnetic activity for both escape paths, but with plasma mantle total O^+ flux typically a factor of 3 higher than in the magnetosheath. The black dashed line is the least-squares fit to the plasma mantle data, and its formula will be presented and discussed in Sect. 4. For quiet times ($Kp \approx 1$), the total O^+ escape rate (considering the plasma mantle route) is $\sim 6 \times 10^{25}\,s^{-1}$, whereas for the highest geomagnetic activity conditions (average $Kp \approx 7$) the rate is $\sim 10^{26}\,s^{-1}$.

As seen in Fig. 5, there are large variations in the measured scaled fluxes for a given Kp value. Therefore, the estimated values given above, for which the whole range of flux values were considered, can be seen as average O^+ escape rates. To get an estimate of how high (and low) the escape rate may be for a given geomagnetic condition, we instead only consider the flux data over the 80th (below the 20th) percentile within each segment. The results give an upper and lower estimate of the range of escape rates for a given geomagnetic condition, also shown in Fig. 7 as coloured areas; light blue is the plasma mantle route and light red is the dayside magnetosheath route. The upper and lower estimates typically have the same dependence on Kp as the average escape rates, but are significantly higher or lower, which is consistent with the large standard deviations observed in the scaled fluxes (Fig. 5)

4 Discussion

4.1 Kp dependence

The total O^+ escape from the terrestrial magnetosphere as a function of geomagnetic activity for two different escape routes (via the plasma mantle and subsequent escape in the far tail and via open magnetic field lines directly from the cusp into the high-latitude magnetosheath) has been statistically investigated and quantified. As expected, there is a clear increase in the O^+ escape with increased Kp index for both escape routes, as shown in Fig. 7. In the same figure, the least-squares fit of O^+ escape via the plasma mantle (superscript pm) as a function of Kp is an exponential function given by

$$\Phi_{O^+}^{pm}(Kp) = 3.9 \times 10^{24} \exp(0.45\,Kp), \quad [s^{-1}]. \tag{1}$$

The O^+ escape directly from the cusp into the high-latitude magnetosheath (superscript ms) is typically a factor of 3 smaller than the escape via the plasma mantle for a given geomagnetic activity condition, such that $\Phi_{O^+}^{ms} \approx \Phi_{O^+}^{pm}/3$. These expressions can be extrapolated to predict average escape fluxes for the very strongest geomagnetic storms: $\Phi_{O^+}^{pm}(Kp = 9) = 2.25 \times 10^{26}\,s^{-1}$ and a total escape of $3 \times 10^{26}\,s^{-1}$, if also considering the escape directly from the cusp into the dayside magnetosheath. Note that this value is an average including both hemispheres, i.e. the summer and winter hemispheres, because the Cluster trajectory with a 90° inclination was nearly north–south symmetric during 2001–2005.

The exponential dependence of O^+ escape on Kp ($\Phi \propto \exp(0.45\,Kp)$) is similar and consistent with an O^+ outflow

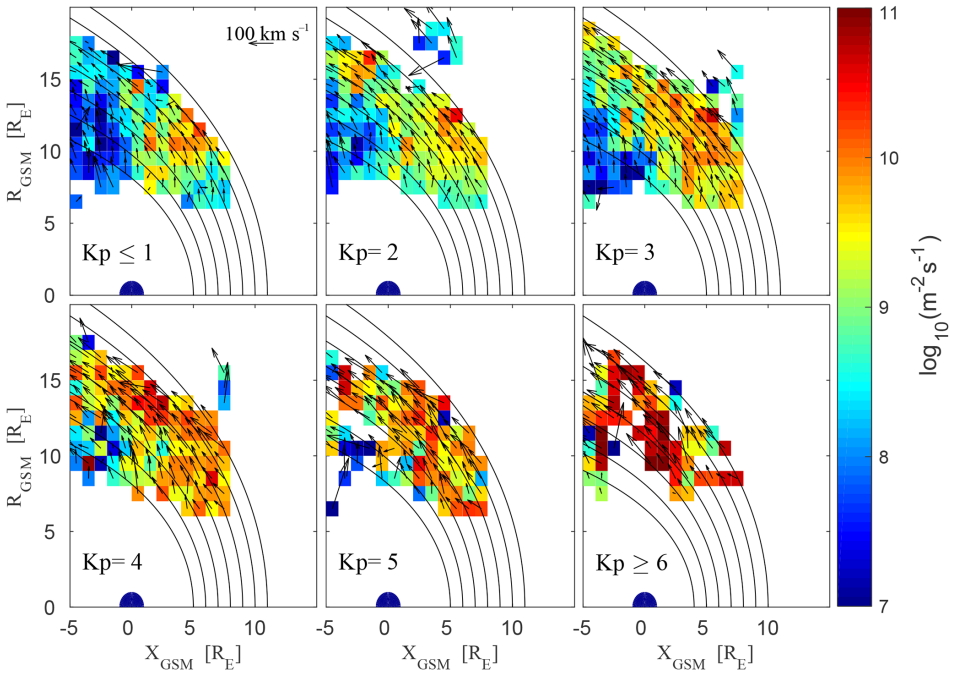

Figure 6. The spatial distribution of plasma mantle O$^+$ flux in cylindrical coordinates, (X_{gse}, $R_{gse} = (Y_{gse}^2 + Z_{gse}^2)^{1/2}$), for periods of different geomagnetic conditions: Kp = (0, 1), Kp = 2, Kp = 3, Kp = 4, Kp = 5, and Kp = (6, 7, 8). The colour bar defines the average flux intensity, and the arrows represent the average O$^+$ bulk velocity.

study by Yau et al. (1988), who mapped and integrated high-invariant latitude ($> 56°$) O$^+$ outflows using data obtained by Dynamics Explorer 1 (DE1) for an O$^+$ energy range of 0.01–17 keV. They found an $\propto \exp(0.50\,\mathrm{Kp})$ relation for a Kp range from 0 to 6. The total O$^+$ flux in their study was about a factor of 2.3 larger than the results presented in our study, given a certain condition on the geomagnetic activity. It makes no real sense to further compare our results with those of Yau et al. (1988), since the lower limit of the invariant latitude of 56° includes the whole polar cap, cusp, and auroral region. Pollock et al. (1990) calculated the total O$^+$ outflow for the cusp region specifically, also using data provided by instruments on-board DE1, and obtained a flux rate of 2×10^{25} s^{-1} without investigating any dependence on geomagnetic activity. This outflow is similar to the escape rates that we present in this study for average geomagnetic conditions, suggesting that a significant part of the O$^+$ cusp outflow will eventually escape, in principle via route 2 or 3 (Fig. 1).

4.2 EUV and seasonal effects

According to Cully et al. (2003), Peterson et al. (2008), and Maes et al. (2015), EUV flux is another leading factor that controls the escape flux, with much higher EUV flux associated with the summer hemisphere than the winter hemisphere. Figure 7 shows a wide range of escaping flux for a given Kp value, with 1 to 2 orders of magnitude difference between the lower (below the 20th percentile) and the upper (over the 80th percentile) values. This is largely influenced by the influx of the solar EUV to the ionosphere (Moore et al., 1999; Cully et al., 2003; Peterson et al., 2006).

A solid estimate including the EUV dependence must include an estimation of the EUV influx to the ionosphere and the solar zenith angle, but such a formulation is model-dependent since we need to assume an effective latitude. Instead, we use the upper value in Fig. 7 as an estimate of the escape rate from the summer hemisphere.

4.3 Escape rate in the past

By considering the highest 20 % of the values instead of all data points, the O$^+$ loss rate from the cusp and plasma mantle becomes as high as 10^{27} s^{-1} for Kp = 9. This O$^+$ escape rate is 2 orders of magnitude larger than observed for typical average conditions (Nilsson, 2011; Slapak et al., 2013). Considering the evolution of G-type stars (or all main sequence stars), the young Sun was much more active than it is today in terms of higher emission of EUV radiation, faster solar wind, and a faster rotation, with more active sunspots and stronger IMF as a consequence due to a more effective solar dynamo (e.g. Ribas et al., 2005; Wood, 2006). Conditions during major geomagnetic storms are currently sometimes considered as a proxy for normal conditions in the ancient solar system (Krauss et al., 2012), and therefore Eq. (1) and the corresponding expression for the high-latitude mag-

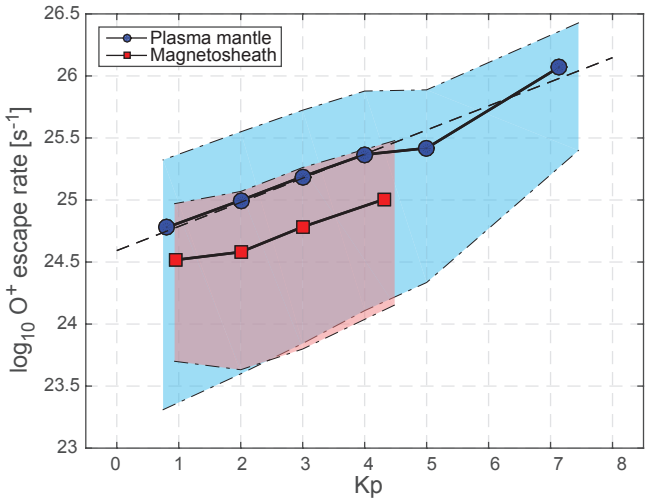

Figure 7. The average O^+ escape rates for the plasma mantle (solid blue line and circles) and the dayside magnetosheath (solid red line and squares) as a function of Kp. The dashed black line is a least-squares fit to the average escape rates for the plasma mantle. The thin dot-dashed lines correspond to estimated upper and lower O^+ escape rates in the plasma mantle (blue area) and the magnetosheath (red) based on the highest and lowest flux values observed under the different geomagnetic conditions.

netosheath can be used to estimate atmospheric loss during ancient epochs. However, a possible issue is that the relative abundance of oxygen in the atmosphere has changed considerably over time (e.g. Holland, 2006; Lyons et al., 2014), and consequently the question arises of how this change affects the O^+ outflow and escape over time. Measurements at Mars and Venus, which have CO_2-dominant atmospheres, show oxygen-dominated upper ionospheres and outflows (Lundin, 2011, and references therein). This indicates that the relative abundance of oxygen and even the composition of the atmosphere as a whole will not significantly affect the upper ionosphere. Therefore the upper ionosphere of the ancient Earth was most probably O^+-dominated independent of the oxygen abundance in the atmosphere, allowing us to extrapolate our result for present Earth to ancient times.

If $\mathrm{Kp}(t)$ is the average geomagnetic activity as a function of time, then the total loss L of O^+ from a time t_0 until the present day t_n can be expressed as

$$L = \int_{t_0}^{t_n} \Phi(\mathrm{Kp}(t))\mathrm{d}t, \tag{2}$$

with Φ given by Eq. (1). We do not know how the average Kp has changed explicitly over time, but we can make rough estimates of the total O^+ escape. Assuming that $\mathrm{Kp} = 10$ four billion years ago and decreasing linearly with time (exponential decay in terms of geomagnetic deviation in nT), the total O^+ loss becomes $\sim 4.8 \times 10^{17}$ kg, corresponding to 40 % of today's total oxygen mass in the atmosphere. Krauss et al. (2012) investigated an X17.2 flare on 28 October 2003 during the "Halloween period" (Rosenqvist et al., 2005) and concluded that the conditions served as a proxy for the Sun at the age of 2.3 billion years. Using this as a reference time and $\mathrm{Kp} = 9$ as associated with the Halloween events and integrating over four billion years, we get a total O^+ loss that is 1.3 times the total oxygen mass in the atmosphere today. Both estimates give a total O^+ loss of the same order as atmospheric oxygen content at the present time. These estimates assume that all ions detected in the O^+ mass channel of the CODIF spectrometer are indeed O^+. However, given the finite mass resolution of the instrument ($m/\Delta m \sim 5-7$), N^+ ions could also be part of the population. N^+ ions have been observed to take substantial proportions in the outflow during very active periods (Hamilton et al., 1988; Christon et al., 2002). A better understanding of and insight into the solar and geomagnetic conditions on geological timescales is needed in order to further investigate this matter and is left for future consideration. A systematic survey of the outflows using high mass-resolution instrumentation, as with the recently proposed ESA ESCAPE mission, would allow a detailed investigation, a separation of the O^+ and N^+ escape rates, and a study of their links to the solar and magnetospheric activity.

5 Conclusions

We have estimated the typical O^+ escape in high-latitude and high-altitude regions via the plasma mantle and dayside magnetosheath and found that it increases exponentially as $\exp(0.45\,\mathrm{Kp})$; this is consistent with earlier observed O^+ outflow dependences on Kp at lower altitudes (Yau et al., 1988). The dominant escape route is via the plasma mantle and is quantitatively given by $\Phi_{O^+}^{pm}(\mathrm{Kp}) = 3.9 \times 10^{24} \exp(0.45\,\mathrm{Kp})$ [s^{-1}]. Escape directly from the cusp into the dayside magnetosheath is smaller (by about a factor of 3) but significant. An extrapolation of the result suggests an average oxygen ion escape of $3 \times 10^{26}\,s^{-1}$ for conditions when $\mathrm{Kp} = 9$. Estimates of the total O^+ escape [kg] since the Earth was young until today indicate that it is roughly equal to the amount of the present atmospheric oxygen content.

Data availability. All Cluster data are freely accessible and retrieved from the Cluster Science Archive (https://www.cosmos.esa.int/web/csa). The geomagnetic activity data (Kp indices) are retrieved from the GFZ Adolf Schmidt Observatory, Niemegk (http://www.gfz-potsdam.de/en/kp-index/).

Competing interests. The authors declare that they have no conflict of interest.

Acknowledgements. We want to thank the Swedish National Space Board, the Graduate School of Space Technology and the Swedish Institute of Space Physics for financial support. The authors also want to thank to the Cluster CODIF and FGM instrument teams for providing data that can be freely retrieved from the Cluster Science Archive. The Kp indices are provided by the GFZ Adolf Schmidt Observatory in Niemegk, Germany.

The topical editor, Georgios Balasis, thanks two anonymous referees for help in evaluating this paper.

References

Airapetian, V. S. and Usmanov, A. V.: Reconstructing the solar wind from its early history to current epoch, Astrophys. J. Lett., 817, L24, https://doi.org/10.3847/2041-8205/817/2/L24, 2016.

André, M., Crew, G. B., Peterson, W. K., Persoon, A. M., Pollock, C. J., and Engebretson, M. J.: Ion heating by broadband low-frequency waves in the cusp/cleft, J. Geophys. Res., 95, 20809–20823, https://doi.org/10.1029/JA095iA12p20809, 1990.

Balogh, A., Carr, C. M., Acuña, M. H., Dunlop, M. W., Beek, T. J., Brown, P., Fornacon, K.-H., Georgescu, E., Glassmeier, K.-H., Harris, J., Musmann, G., Oddy, T., and Schwingenschuh, K.: The Cluster Magnetic Field Investigation: overview of in-flight performance and initial results, Ann. Geophys., 19, 1207–1217, https://doi.org/10.5194/angeo-19-1207-2001, 2001.

Baumjohann, W., Paschmann, G., and Cattell, C. A.: Average plasma properties in the central plasma sheet, J. Geophys. Res., 94, 6597–6606, https://doi.org/10.1029/JA094iA06p06597, 1989.

Bouhram, M., Malingre, M., Jasperse, J. R., Dubouloz, N., and Sauvaud, J.-A.: Modeling transverse heating and outflow of ionospheric ions from the dayside cusp/cleft. 2 Applications, Ann. Geophys., 21, 1773–1791, https://doi.org/10.5194/angeo-21-1773-2003, 2003.

Bouhram, M., Klecker, B., Paschmann, G., Haaland, S., Hasegawa, H., Blagau, A., Rème, H., Sauvaud, J.-A., Kistler, L. M., and Balogh, A.: Survey of energetic O^+ ions near the dayside mid-latitude magnetopause with Cluster, Ann. Geophys., 23, 1281–1294, https://doi.org/10.5194/angeo-23-1281-2005, 2005.

Christon, S. P., Mall, U., Eastman, T. E., Gloeckler, G., Lui, A. T. Y., McEntire, R. W., and Roelof, E. C.: Solar cycle and geomagnetic N^{+1}/O^{+1} variation in outer dayside magnetosphere: Possible relation to topside ionosphere, Geophys. Res. Lett., 29, 1058, https://doi.org/10.1029/2001GL013988, 2002.

Cully, C. M., Donovan, E. F., Yau, A. W., and Arkos, G. G.: Akebono/Suprathermal Mass Spectrometer observations of low-energy ion outflow: Dependence on magnetic activity and solar wind conditions, J. Geophys. Res.-Space, 108, 1093, https://doi.org/10.1029/2001JA009200, 2003.

Engwall, E., Eriksson, A. I., Cully, C. M., André, M., Torbert, R., and Vaith, H.: Earth's ionospheric outflow dominated by hidden cold plasma, Nat. Geosci., 2, 24–27, https://doi.org/10.1038/ngeo387, 2009.

Escoubet, C. P., Fehringer, M., and Goldstein, M.: *Introduction* The Cluster mission, Ann. Geophys., 19, 1197–1200, https://doi.org/10.5194/angeo-19-1197-2001, 2001.

Güdel, M.: The Sun in time: activity and environment, Living Rev. Sol. Phys., 4, 1–137, https://doi.org/10.12942/lrsp-2007-3, 2007.

Haaland, S., Eriksson, A. I., Engwall, E., Lybekk, B., Nilsson, H., Pedersen, A., Svenes, K., Förster, M., Li, K., Johnsen, C., and Østgaard, N.: Estimating the capture and loss of cold plasma from ionospheric outflow, J. Geophys. Res., 117, A07311, https://doi.org/10.1029/2012JA017679, 2012.

Hamilton, D. C., Gloeckler, G., Ipavich, F. M., Wilken, B., and Stuedemann, W.: Ring current development during the great geomagnetic storm of February 1986, J. Geophys. Res., 93, 14343–14355, https://doi.org/10.1029/JA093iA12p14343, 1988.

Holland, H. D.: The oxygenation of the atmosphere and oceans, Phil. Trans. R. Soc. B, 361, 903–915, https://doi.org/10.1098/rstb.2006.1838, 2006.

Kistler, L. M. and Mouikis, C. G.: The inner magnetosphere ion composition and local time distribution over a solar cycle, J. Geophys. Res., 121, 2009–2032, https://doi.org/10.1002/2015JA021883, 2016.

Kistler, L. M., Mouikis, C. G., Cao, X., Frey, H., Klecker, B., Dandouras, I., Korth, A., Marcucci, M. F., Lundin, R., McCarthy, M., Friedel, R., and Lucek, E.: Ion composition and pressure changes in storm time and nonstorm substorms in the vicinity of the near-Earth neutral line, J. Geophys. Res., 111, A11222, https://doi.org/10.1029/2006JA011939, 2006.

Kistler, L. M., Mouikis, C. G., Klecker, B., and Dandouras, I.: Cusp as a source for oxygen in the plasma sheet during geomagnetic storms, J. Geophys. Res., 115, A03209, https://doi.org/10.1029/2009JA014838, 2010.

Krauss, S., Fichtinger, B., Lammer, H., Hausleitner, W., Kulikov, Yu. N., Ribas, I., Shematovich, V. I., Bisikalo, D., Lichtenegger, H. I. M., Zaqarashvili, T. V., Khodachenko, M. L., and Hanslmeier, A.: Solar flares as proxy for the young Sun: satellite observed thermosphere response to an X17.2 flare of Earth's upper atmosphere, Ann. Geophys., 30, 1129–1141, https://doi.org/10.5194/angeo-30-1129-2012, 2012.

Liao, J., Kistler, L. M., Mouikis, C. G., Klecker, B., Dandouras, I., and Zhang, J.-C.: Statistical study of O^+ transport from the cusp to the lobes with Cluster CODIF data, J. Geophys. Res., 115, A00J15, https://doi.org/10.1029/2010JA015613, 2010.

Liao, J., Kistler, L. M., Mouikis, C. G., Klecker, B., and Dandouras, I.: Acceleration of O^+ from the cusp to the plasma sheet, J. Geophys. Res.-Space, 120, 1022–1034, https://doi.org/10.1002/2014JA020341, 2015.

Lundin, R.: Ion acceleration and outflow from Mars and Venus: An overview, Space Sci. Rev., 162, 309–334, https://doi.org/10.1007/s11214-011-9811-y, 2011.

Lyons, T. W., Reinhard, C. T., and Planavsky, N. J.: The rise of oxygen in Earth's early ocean and atmosphere, Nature, 506, 307–315, https://doi.org/10.1038/nature13068, 2014.

Maes, L., Maggiolo, R., De Keyser, J., Dandouras, I., Fear, R. C., Fontaine, D., and Haaland, S.: Solar illumination control of ionospheric outflow above polar cap arcs, Geophys. Res. Lett., 42, 1304–1311, https://doi.org/10.1002/2014GL062972, 2015.

Marcucci, M. F., Bavassano Cattaneo, M. B., Pallocchia, M., Amata, E., Bruno, R., Di Lellis, A. M., Formisano, V., Rème, H., Bosqued, J. M., Dandouras, I., Sauvoud, J. A., Kistler, L. M., Moebius, E., Klecker, B., Carlson, C. W., Parks, G. K., McCarthy, M., Korth, A., Lundin, R., and Balogh, A.: Energetic magnetospheric oxygen in the magnetosheath and its response to IMF orientation: Cluster observations, J. Geophys. Res., 109, A07203, https://doi.org/10.1029/2003JA010312, 2004.

Moore, T. E., Lundin, R., Alcayde, D., André, M., Ganguli, S. B., Temerin, M., and Yau, A.: Source processes in the high-latitude ionosphere, Space Sci. Rev., 88, 7–84, https://doi.org/10.1023/A:1005299616446, 1999.

Nilsson, H.: Heavy ion energization, transport, and loss in the Earth's magnetosphere, in: The Dynamic Magnetosphere, edited by: Liu, W. and Fujimoto, M., https://doi.org/10.1007/978-94-007-0501-2_17, IAGA, Springer, 2011.

Nilsson, H., Yamauchi, M., Eliasson, L., Norberg, O., and Clemmons, J.: Ionospheric signature of the cusp as seen by incoherent scatter radar, J. Geophys. Res., 101, 10947–10963, https://doi.org/10.1029/95JA03341, 1996.

Nilsson, H., Waara, M., Arvelius, S., Marghitu, O., Bouhram, M., Hobara, Y., Yamauchi, M., Lundin, R., Rème, H., Sauvaud, J.-A., Dandouras, I., Balogh, A., Kistler, L. M., Klecker, B., Carlson, C. W., Bavassano-Cattaneo, M. B., and Korth, A.: Characteristics of high altitude oxygen ion energization and outflow as observed by Cluster: a statistical study, Ann. Geophys., 24, 1099–1112, https://doi.org/10.5194/angeo-24-1099-2006, 2006.

Nilsson, H., Barghouthi, I. A., Slapak, R., Eriksson, A., and André, M.: Hot and cold ion outflow: spatial distribution of ion heating, J. Geophys. Res., 117, A11201, https://doi.org/10.1029/2012JA017974, 2012.

Norqvist, P., André, M., Eliasson, L., Eriksson, A. I., Blomberg, L., Lühr, H., and Clemmons, J. H.: Ion cyclotron heating in the dayside magnetosphere, J. Geophys. Res., 101, 13179–13194, https://doi.org/10.1029/95JA03596, 1996.

Nose, M., Taguchi, S., Hosokawa, K., Christon, S. P., McEntire, R. W., Moore, T. E., and Collier, M. R.: Overwhelming O^+ contribution to the plasma sheet energy density during the October 2003 superstorm: Geotail/EPIC and IMAGE/LENA observations, J. Geophys. Res., 110, A09S24, https://doi.org/10.1029/2004JA010930, 2005.

Ogawa, Y., Fujii, R., Buchert, S. C., Nozawa, S., and Ohtani, S.: Simultaneous EISCAT Svalbard radar and DMSP observations of ion upflow in the dayside polar ionosphere, J. Geophys. Res., 108, 1101, https://doi.org/10.1029/2002JA009590, 2003.

Peterson, W. K., Collin, H. L., Yau, A. W., and Lennartsson, O. W.: Polar/Toroidal Imaging Mass-Angle Spectrograph observations of suprathermal ion outflow during solar minimum conditions, J. Geophys. Res., 106, 6059–6066, https://doi.org/10.1029/2000JA003006, 2001.

Peterson, W. K., Collin, H. L., Lennartsson, O. W., and Yau, A. W.: Quiet time solar illumination effects on the fluxes and characteristic energies of ionospheric outflows, J. Geophys. Res., 111, A11S05, https://doi.org/10.1029/2005JA011596, 2006.

Peterson, W. K., Andersson, L., Callahan, B. C., Collin, H. L., Scudder, J. D., and Yau, A. W.: Solar-minimum quiet time ion energization and outflow in dynamic boundary related coordinates, J. Geophys. Res., 113, A07222, https://doi.org/10.1029/2008JA013059, 2008.

Pollock, C. J., Chandler, M. O., Moore, T. E., Waite Jr., J. H., Chappell, C. R., and Gurnett, D. A.: A survey of upwelling ion event characteristics, J. Geophys. Res., 95, 18969–18980, https://doi.org/10.1029/JA095iA11p18969, 1990.

Rème, H., Aoustin, C., Bosqued, J. M., Dandouras, I., Lavraud, B., Sauvaud, J. A., Barthe, A., Bouyssou, J., Camus, Th., Coeur-Joly, O., Cros, A., Cuvilo, J., Ducay, F., Garbarowitz, Y., Medale, J. L., Penou, E., Perrier, H., Romefort, D., Rouzaud, J., Vallat, C., Alcaydé, D., Jacquey, C., Mazelle, C., d'Uston, C., Möbius, E., Kistler, L. M., Crocker, K., Granoff, M., Mouikis, C., Popecki, M., Vosbury, M., Klecker, B., Hovestadt, D., Kucharek, H., Kuenneth, E., Paschmann, G., Scholer, M., Sckopke, N., Seidenschwang, E., Carlson, C. W., Curtis, D. W., Ingraham, C., Lin, R. P., McFadden, J. P., Parks, G. K., Phan, T., Formisano, V., Amata, E., Bavassano-Cattaneo, M. B., Baldetti, P., Bruno, R., Chionchio, G., Di Lellis, A., Marcucci, M. F., Pallocchia, G., Korth, A., Daly, P. W., Graeve, B., Rosenbauer, H., Vasyliunas, V., McCarthy, M., Wilber, M., Eliasson, L., Lundin, R., Olsen, S., Shelley, E. G., Fuselier, S., Ghielmetti, A. G., Lennartsson, W., Escoubet, C. P., Balsiger, H., Friedel, R., Cao, J.-B., Kovrazhkin, R. A., Papamastorakis, I., Pellat, R., Scudder, J., and Sonnerup, B.: First multispacecraft ion measurements in and near the Earth's magnetosphere with the identical Cluster ion spectrometry (CIS) experiment, Ann. Geophys., 19, 1303–1354, https://doi.org/10.5194/angeo-19-1303-2001, 2001.

Ribas, S., Guinan, E. F., Güdel, M., and Audard, M.: Evolution of the solar activity over time and effects on planetary atmospheres. I. High-energy irradiances (1–1700 Å), Astrophys. J., 622, 680–694, https://doi.org/10.1086/427977, 2005.

Rosenqvist, L., Opgenoorth, H., Buchert, S., McCrea, I., Amm, O., and Lathuillere, C.: Extreme solar-terrestrial events of October 2003: High-latitude and Cluster observations of the large geomagnetic disturbances on 30 October, J. Geophys. Res., 110, A09S23, https://doi.org/10.1029/2004JA010927, 2005.

Shue, J.-H., Chao, J., Fu, H., Russell, C., Song, P., Khurana, K., and Singer, H.: A new functional form to study the solar wind control of the magnetopause size and shape, J. Geophys. Res., 102, 9497–9511, https://doi.org/10.1029/97JA00196, 1997.

Slapak, R., Nilsson, H., Waara, M., André, M., Stenberg, G., and Barghouthi, I. A.: O^+ heating associated with strong wave activity in the high altitude cusp and mantle, Ann. Geophys., 29, 931–944, https://doi.org/10.5194/angeo-29-931-2011, 2011.

Slapak, R., Nilsson, H., Westerberg, L. G., and Eriksson, A.: Observations of oxygen ions in the dayside magnetosheath associated with southward IMF, J. Geophys. Res., 117, A07218, https://doi.org/10.1029/2012JA017754, 2012.

Slapak, R., Nilsson, H., and Westerberg, L. G.: A statistical study on O^+ flux in the dayside magnetosheath, Ann. Geophys., 31, 1005–1010, https://doi.org/10.5194/angeo-31-1005-2013, 2013.

Slapak, R., Nilsson, H., Westerberg, L. G., and Larsson, R.: O^+ transport in the dayside magnetosheath and its dependence on the IMF direction, Ann. Geophys., 33, 301–307, https://doi.org/10.5194/angeo-33-301-2015, 2015.

Song, P. and Russell, C. T.: Model of the formation of the low-latitude boundary layer for strongly northward interplanetary magnetic field, J. Geophys. Res., 97, 1411–1420, https://doi.org/10.1029/91JA02377, 1992.

Waara, M., Slapak, R., Nilsson, H., Stenberg, G., André, M., and Barghouthi, I. A.: Statistical evidence for O+ energization and outflow caused by wave-particle interaction in the high altitude cusp and mantle, Ann. Geophys., 29, 945–954, https://doi.org/10.5194/angeo-29-945-2011, 2011.

Wood, B. E.: The solar wind and the Sun in the past, Space Sci. Rev., 126, 3–14, https://doi.org/10.1007/s11214-006-9006-0, 2006.

Yau, A. W. and André, M.: Sources of ion outflow in the high latitude ionosphere, Space Sci. Rev., 80, 1–25, https://doi.org/10.1023/A:1004947203046, 1997.

Yau, A. W., Peterson, W. K., and Shelley, E. G.: Quantitative parametrization of energetic ionospheric ion outflow, Geophys. Monogr. Ser., 44, 211–217, https://doi.org/10.1029/GM044p0211, 1988.

Young, D. T., Balsiger, H., and Geiss, J.: Correlations of magnetospheric ion composition with geomagnetic and solar activity, J. Geophys. Res., 87, 9077–9096, https://doi.org/10.1029/JA087iA11p09077, 1982.